



HAL
open science

Direct measurement of total emissivities at cryogenic temperatures: Application to satellite coatings

Philippe Hervé, Nicolas Rambure, Abdelkader Sadou, David Ramel, Laurent Francou, P. Delouard, Emmanuel Gavila

► **To cite this version:**

Philippe Hervé, Nicolas Rambure, Abdelkader Sadou, David Ramel, Laurent Francou, et al.. Direct measurement of total emissivities at cryogenic temperatures: Application to satellite coatings. *Cryogenics*, 2008, 48 (11-12), pp.463-468. 10.1016/j.cryogenics.2008.07.007 . hal-00399898

HAL Id: hal-00399898

<https://hal.science/hal-00399898>

Submitted on 8 Nov 2018

HAL is a multi-disciplinary open access archive for the deposit and dissemination of scientific research documents, whether they are published or not. The documents may come from teaching and research institutions in France or abroad, or from public or private research centers.

L'archive ouverte pluridisciplinaire **HAL**, est destinée au dépôt et à la diffusion de documents scientifiques de niveau recherche, publiés ou non, émanant des établissements d'enseignement et de recherche français ou étrangers, des laboratoires publics ou privés.

Public Domain

Direct measurement of total emissivities at cryogenic temperatures: Application to satellite coatings

P. Herve^a, N. Rambure^a, A. Sadou^{a,*}, D. Ramel^a, L. Francou^a, P. Delouard^b, E. Gavila^c

^a Université Paris 10, 1 Chemin Desvallières, 92410 Ville d'Avray, France

^b Contraves Space AG, Schaffhauserstrasse, 580 CH-8052 Zürich, Switzerland

^c Alcatel Space, 100 boulevard du Midi, BP99-06322 Cannes La Bocca, France

This paper presents a direct measurement method for optical properties of different materials at cryogenic temperatures from 20 K to 200 K. It has been developed within the framework of the design of Planck program. Planck is a satellite of the European Space Agency (ESA) that will be launched in 2008. The scientific goal of the Planck mission is to make observations of the temperature anisotropy and polarisation of the Cosmic Microwave Background. The equivalent temperature of the observed radiation is about 3 K and the telescope baffle temperature should not exceed 60 K in order to work properly. The large Planck telescope is passively cooled by radiating to the Deep Space, so that a good knowledge of the thermo-optical properties of its coating is of utmost importance for thermal modelling. However, up to now, few measurements have been done at such low temperatures. We derived a direct measurement method for the total directional emissivity of various coatings of interest for satellites applications. The effective spectral range chosen the measurements covers 6–800 μm . We will describe the design of the measurement apparatus and present results for several coatings.

1. Introduction

Planck satellite that should be launched by ESA in 2007 will “look back to the dawn of time”, close to the Big Bang, and will observe the most ancient radiation in the Universe whose average temperature is 2.73 K [1].

To perform its mission, the satellite, inserted into the Lagrange-2 point of the Earth–Sun system, must comply with several technical requirements. Thus, not to disturb the measuring process, temperature of the satellite telescope must remain stable around 50 K. This temperature is passively obtained by the radiation of the telescope toward deep space with the cold areas constantly shadowed from the sun by the service module. The most emissive coating should be chosen for the telescope outer elements in order to maximize the radiated flux.

LEEE was asked by CONTRAVES SPACE (Planck telescope structure responsible), under supervision of ALCATEL SPACE (Planck prime contractor), to study the emissivity of different coatings in the temperature range 40–200 K.

In order to make total emissivity measurements for coatings, we have to consider that 97% of the radiant energy of bodies around 40 K is located in the far infrared at wavelengths between 40 μm and 800 μm . It is of little use for on Earth applications to

work in this spectral range as the propagation is strongly attenuated by the numerous absorption bands of atmospheric water. That is why common infrared applications work in the 1–12 μm spectral band which covers most of the radiant energy at temperatures between 200 K and 3000 K. For satellite applications, however, there are no such transmission gaps and, when studying emission from very cold bodies, it is necessary to determine optical properties of coatings in the far infrared.

We will present here the method and the equipment developed by LEEE for this project. The temperature range for experiments is between 10 K and 200 K. The spectral range is between 6 μm and 800 μm .

2. Measurement method

To measure emissivity of opaque materials, we can use three different methods:

- (1) by direct measurement of emissivity ε (directional or hemispherical, spectral or total);
- (2) by measurement of the reflectivity ρ , knowing the relationship $\varepsilon = 1 - \rho$ [2];
- (3) by calorimetric measurements [3–5].

With a calorimetric measurement, one obtains total hemispherical emissivity. It is a relatively simple method to implement and

* Corresponding author. Tel./fax: +33 1 47097013/1645.

E-mail addresses: pherve@u-paris10.fr (P. Herve), asadou@univ-ubs.fr (A. Sadou).

Nomenclature

Cte	apparatus function
L^0	radiation total intensity of the blackbody ($\text{W m}^{-2} \text{sr}^{-1}$)
Mb	measurement on blackbody
Ms	measurement on sample
T	temperature (K)
ε	total emissivity
ε_λ	spectral emissivity
ε_T	total emissivity at temperature, T
Δ	temperature difference between two points
λ	wavelength (m)

ρ	total reflectivity
ρ_λ	spectral reflectivity
ρ_T	total reflectivity at temperature T
σ	constant of Stefan–Boltzmann ($\text{W/m}^2 \text{K}^4$)
Subscripts	
J	index of iteration
c	chopper
w	wall
B	blackbody

widely used at ambient temperature but, in previous measurement campaigns and for temperatures lower than 100 K, we got heat leakages that induced parasitic phenomena of the same order of magnitude as those of interest.

Indirect measurements could be a good alternative to obtain emissivity but, as the coatings to be experimented are thin layers of dielectric materials deposited on metallic substrate, they become semi-transparent in the far infrared. Such phenomenon induces multiple reflections at the interfaces air-coating and metal-coating, resulting in a non-validity of the relationship $\varepsilon = 1 - \rho$. We then concluded that, in this very situation, direct emissivity measurement was the right choice.

The main flaw lies in that the emitted radiation of the sample at such low temperatures is very faint compared to the background radiation received by the detector. In order to minimize the background radiation, we use a vacuum chamber cooled by liquid nitrogen (77 K). In addition, we use a lock-in amplifier with a chopper that modulates the component of the signal coming from the inner part of the vacuum chamber and eliminates the outside background radiation. When the detector sees the sample between two rotating blades of the chopper, the signal is the sum of the thermal radiation emitted by the sample itself, added to the radiation coming from all the parts of the vacuum chamber (with emissivity $\varepsilon_w \approx 1$ and a radiant equivalent temperature $T_w = 80$ K) that is reflected by the sample plus the thermal radiation emitted by the optics (with emissivity ε_o , reflectivity ρ_o and temperature T_o). When a chopper blade (with emissivity ε_c and temperature T_c) hides the sample, the detector receives the sum of the thermal radiation emitted and reflected by the blade, which value can be higher than the useful signal. The lock-in amplifier calculates the difference between the two above signals.

The method proposed operates by subtracting the signals obtained for two different sample temperatures T_A and T_B . Measuring the radiation of the sample and of a blackbody for the same two temperatures, we get the following relationships:

(1) Intensity measurement of the sample at temperature T_1 .

$$Ms_A = Cte^*(\varepsilon_{T_A}\rho_o\sigma T_A^4 - \varepsilon_c\sigma T_c^4 + \rho_{T_A}\rho_o\varepsilon_w\sigma T_w^4 - \rho_c\varepsilon_w\sigma T_w^4 + \varepsilon_o\sigma T_o^4) \quad (1)$$

(2) Intensity measurement of the sample at temperature T_2 .

$$Ms_B = Cte^*(\varepsilon_{T_B}\rho_o\sigma T_B^4 - \varepsilon_c\sigma T_c^4 + \rho_{T_B}\rho_o\varepsilon_w\sigma T_w^4 - \rho_c\varepsilon_w\sigma T_w^4 + \varepsilon_o\sigma T_o^4) \quad (2)$$

(3) Intensity measurement of the blackbody at temperature T_1

$$Mb_A = Cte^*(\rho_o\sigma T_A^4 - \varepsilon_c\sigma T_c^4 - \rho_c\varepsilon_w\sigma T_w^4 + \varepsilon_o\sigma T_o^4) \quad (3)$$

(4) Intensity measurement of the blackbody at T_2

$$Mb_B = Cte^*(\rho_o\sigma T_B^4 - \varepsilon_c\sigma T_c^4 - \rho_c\varepsilon_w\sigma T_w^4 + \varepsilon_o\sigma T_o^4) \quad (4)$$

As we could check (see Section 4) that temperature of optical components does not change during the time of measurement the term $\varepsilon_o\sigma T_o^4$ is in all the equation. We have four equations for nine unknown parameters. To solve this system, several methods can be used, with their benefits and drawbacks conditioned by the assumptions we have to make. Combining Eq. (1) to Eq. (4), we then obtain the following formula.

$$\varepsilon_{T_B} = \varepsilon_{T_A}(T_A/T_B)^4 + \left(1 - (T_A/T_B)^4\right) \frac{(Ms_B - Ms_A)}{(Mb_B - Mb_A)} - (\rho_{T_B} - \rho_{T_A})\varepsilon_w(T_w/T_B)^4 \quad (5)$$

For evaluation of emissivity ε_{T_B} the first and the last terms must be known or negligible. Results of measurements that had been previously conducted on the same Planck samples at the LEMTA laboratory (Laboratoire d'Énergétique et de Mécanique Théorique et Appliquée; ENSEM; Nancy, France) showed that ρ_λ presents little variation with T in the range 40–300 K [6]. Such a result implies that $\rho_T\varepsilon_w\sigma T_w^4 = \pi \int_0^\infty \rho_\lambda(T)\varepsilon_w L_{\lambda,T_w}^0 d\lambda$ remains nearly constant with T , i.e. $\rho_{T_A}\varepsilon_w T_w^4 \approx \rho_{T_B}\varepsilon_w T_w^4$, where L_{λ,T_w}^0 stands for the luminance of a blackbody at the temperature of the vacuum chamber T_w . The influence of this weak temperature dependence on the measurement results is discussed further in Section 4.

Note: Whatever the sample temperature, the reflective part of the signal is due to the chamber wall at 80 K. At this temperature, the wavelength of the maximum of radiated energy is 37 μm and about 97% of energy is contained in the spectral band 20–220 μm . So will be the spectral band of the reflected signal and if, as assumed, $\rho(\lambda, T)$ does not vary with T , the variation of the total emissivity of samples with temperature is only due to the shift in the spectral distribution of the measured radiation energy.

Hereafter we shall write $\rho_{T_A} = \rho_{T_B}$ in Eq. (5). We then obtain the following formula.

$$\varepsilon_{T_B} = (T_A/T_B)^4 \varepsilon_{T_A} + \left(1 - (T_A/T_B)^4\right) \frac{(Ms_B - Ms_A)}{(Mb_B - Mb_A)} \quad (6)$$

We shall then present two methods for solving this equation:

- A “differential method at the lowest temperature”:

To eliminate the influence of the first term with unknown emissivity ε_{T_A} , we can keep for T_A the lowest temperature for which we have got a measurement result ($T_{\min} = 10$ K). As we raise the sample temperature, $\left(\frac{T_{\min}}{T_B}\right)^4 \ll 1$ and the Eq. (6) quickly reduces to:

$$\varepsilon_{T_B} = \frac{(Ms_{T_B} - Ms_{T_{\min}})}{(Mb_{T_B} - Mb_{T_{\min}})} \quad (7)$$

For the temperature T_B close to T_{\min} , the accuracy of the results strongly depends on the hypothesis of the constancy of ρ_λ when T varies, but as the temperature T_B becomes higher than T_w , this assumption is useless because $\left(\frac{T_w}{T_B}\right)^4 \ll 1$.

- An “iterative differential method”:

In Eq. (6), let's take for T_A the temperature of the sample at the immediately preceding measurement step; i.e. $T_A = T_B - \Delta T$. As the difference between T_B and T_A remains lower than in the variant 1, the hypothesis regarding $\rho(\lambda, T)$ should be more easily verified. In return, as there are relatively low differences between the results of two successive measurements steps, the method should be more sensitive to noise.

Let then write $\varepsilon_{T_A} \approx \varepsilon_{T_B}$. Eq. (5) reduces then to

$$\varepsilon_{T_B} = \frac{(Ms_{T_B} - Ms_{T_B - \Delta T})}{(Mb_{T_B} - Mb_{T_B - \Delta T})} \quad (8)$$

Writing $\varepsilon_{T_A} \approx \varepsilon_{T_B}$ is a rough approximation and the result will be refined by iterations through equations system Eq. (9).

If $T_A = T_B - \Delta T$, T_{\min} is the lowest temperature for which we got measurement results and if we define "j" as index of iteration, calculation of emissivity is done following equations system Eq. (9):

$$\left. \begin{array}{l} \text{if } j = 1 : \\ \varepsilon_{T_B} = \frac{(Ms_{T_B} - Ms_{T_B - \Delta T})}{(Mb_{T_B} - Mb_{T_B - \Delta T})} \\ \text{else if } 2 \leq j \leq \frac{T_B - T_{\min}}{\Delta T} : \\ \varepsilon_{(T_B)_j} = \left(\frac{T_B - \Delta T}{T_B}\right)^4 \varepsilon_{(T_B - \Delta T)_{j-1}} + \left(1 - \left(\frac{T_B - \Delta T}{T_B}\right)^4\right) \frac{(Ms_{T_B} - Ms_{T_B - \Delta T})}{(Mb_{T_B} - Mb_{T_B - \Delta T})} \end{array} \right\} \quad (9)$$

The last step gives the best evaluation of emissivities. This variant should normally give better results than variant 1, but the reverse can be true with noisy measurement results.

For example to determine emissivity at 50 K for $\Delta T = 10$ and $T_{\min} = 10$ K :

$$\begin{aligned} \varepsilon_{50} &= \frac{(Ms_{50} - Ms_{40})}{(Mb_{50} - Mb_{40})} \text{ for } j = 1 \text{ and } \varepsilon_{50} \\ &= \left(\frac{40}{50}\right)^4 \varepsilon_{40} + \left(1 - \left(\frac{40}{50}\right)^4\right) \frac{(Ms_{50} - Ms_{40})}{(Mb_{50} - Mb_{40})} \text{ for } j = 2 \text{ to } 4. \end{aligned}$$

Details of such iterations are reproduced further in Table 1, Section 4.

3. Experimental apparatus

To cool the samples, we use a two-stage helium refrigerator. The lowest sample temperature that can be obtained with this refrigerator is 8 K.

The sample holder (Fig. 1) is a cylinder directly linked through a rod to the second stage of the helium refrigerator. For each measurement, five different samples can be disposed on the holder. A blackbody, specially designed for the application [7], with its aperture disposed on the optical path of the measurement setup, is positioned at the top of the sample holder. The whole system can be rotated and translated along its axis to allow measuring of the emission of each sample at multiple angles.

Global accuracy of our results depends on the precision of the estimation of the reference emissivity value. The geometry of the cavity of the blackbody has been carefully studied in order to minimize the effects of internal reflections.

With a ray tracing code, we found that the emissivity of the blackbody exceeds 0.996 when the emissivity of the inner coating exceeds 0.3. We used Velvet painting whose emissivity is clearly better than 0.3 for the lowest temperature of interest. So the corresponding error can be neglected in regard of the other sources of error.

A very good thermal conduction is needed to reach such a low temperature as 10 K and an aluminium alloy AA1050 has been chosen for the cylinder and the rod. A 25 W heating resistance stuck on the back of the sample holder is connected to a PID regulator. The very weak calorific capacity at low temperatures of this alloy makes easier the temperature regulation. Moreover, all thermal contacts have been optimised by application of a vacuum grease (Apiezon N).

The sample temperature is controlled by a silicon diode (temperature range 4–500 K with a 0.01 K sensitivity) inserted at the back of the sample holder and the temperature gradient between the blackbody and the samples is checked by a second silicon diode stuck on the back of the former. We found that, whatever the temperature, the measured gradient does not exceed 0.1 K.

The global measurement apparatus is mainly composed of a vacuum chamber enclosing the optical parts (Fig. 2) and of the detection setup.

With a turbo-molecular pump vacuum chamber we get in the chamber a secondary vacuum about 10^{-7} mbar. So we avoid convective heat transfers and selective absorption of radiations by atmospheric water.

To minimize the level of ambient radiation, the sample holder is placed into a double wall enclosure poured with liquid nitrogen. In addition and to minimize reflections, the inner wall has been painted with Velvet black coating. So parasitic radiations in the chamber depend only on the wall temperature.

The global background flux is equivalent to the radiation of a blackbody at 80 K and we checked that it remains very stable and homogeneous when the temperature of the sample varies.

The optical part of the system is composed of:

- (1) a parabolic mirror disposed in front of the samples, which collects the sample signal into a parallel beam;
- (2) a flat mirror that reflects the parallel beam out of the main chamber through the modulator rotating chopper;
- (3) a second parabolic mirror that focalises the beam onto the bolometer detector through a diamond window that has a very flat transmission curve from 6 μm to 800 μm .

All the optical components and their supporting devices are thermally insulated and they are passively cooled down to 80 K.

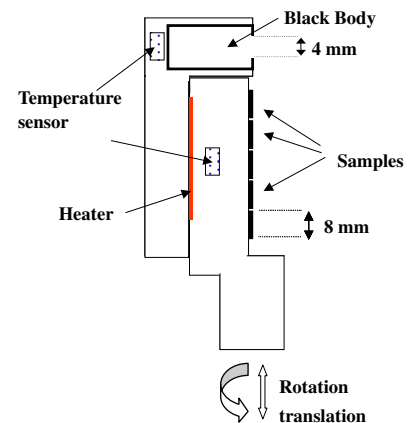


Fig. 1. Schematic diagram of the sample holder.

Table 1
Example of error estimation in "iterative differential method"

T (K)	$\varepsilon_{\text{target}}$	ε_1	$\Delta\varepsilon_1$ (%)	ε_2	$\Delta\varepsilon_2$ (%)	ε_3	$\Delta\varepsilon_3$ (%)	ε_4	$\Delta\varepsilon_4$ (%)
10	0.557								
20	0.606	0.629	2.27						
30	0.690	0.711	2.07	0.695	0.45				
40	0.757	0.789	3.12	0.764	0.66	0.759	0.14		
50	0.810	0.847	3.66	0.823	1.28	0.813	0.27	0.811	0.06

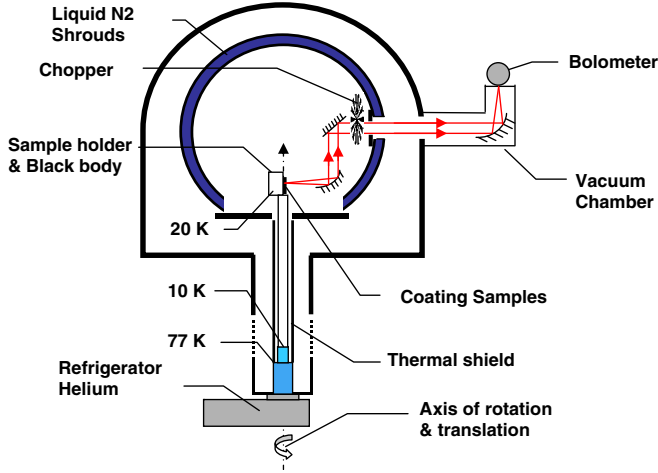


Fig. 2. Schematic diagram of the experimental set-up.

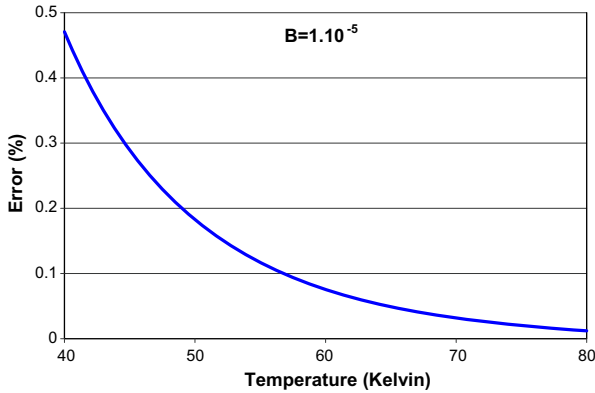


Fig. 3. Systematic error due to a supposed reflectivity variation $\rho_{T,S=80\text{ K}}$.

The detector is a bolometer with an effective bandwidth 2–1000 μm . The detector is cooled at 4.2 K by liquid helium and its associated amplifier NEP is $1.17E^{-13} \text{ W Hz}^{-1/2}$.

To measure the total emissivity, the energy must be collected over the whole optical bandwidth. With gold mirrors, the bolometer and diamond window, we get a very good achromaticity all over the spectral range of interest.

The signal (from the preamplifier of the bolometer) is sent to the lock-in amplifier with a 0.02 Hz equivalent Noise Bandwidth. The difference between the flux received at 40 K and at 20 K is about 10^{-8} W and, as the global noise of our detection system is about $1.6 \times 10^{-14} \text{ W}$, the signal/noise ratio in the calculation method described above is about 10^5 .

The system is cooled for 12 h before beginning the measurements to make sure that all the components are well stabilized at 80 K.

4. Error analysis

There are two main categories of errors that can be considered separately in the global error budget: the systematic one, that results from the assumptions in the calculation method and the experimental one, part of which being random.

To get an evaluation of the systematic error, we use already mentioned (unpublished) results from LEMTA. We use the results $\varepsilon_{\lambda,300}$ on the spectral band 1–600 μm and we suppose that the variation of the spectral emissivity obeys a law $\varepsilon_{\lambda,T} = \varepsilon_{\lambda,300} - B(300 - T)$ with B comprised between 10^{-6} and 5×10^{-5} depending of the coating. From $\varepsilon_{\lambda,T}$, we can integrate the total emissivity

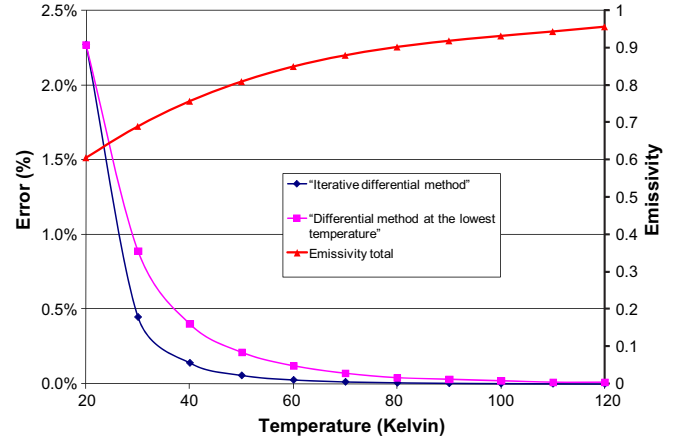


Fig. 4. Comparison of systematic errors for two methods of the calculation “differential method at the lowest temperature” and “iterative differential method”.

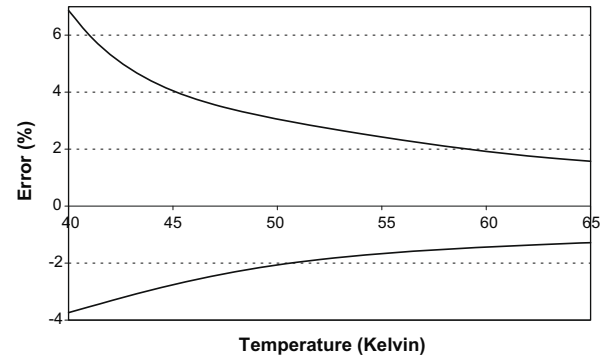


Fig. 5. Estimation of global error.

ε_T and the total reflectivity $\rho_{T,S=80\text{ K}}$ of the coating at T reflecting a signal emitted by a source at 80 K. Thus, we modelize the energy radiated by the sample and by the blackbody for each temperature T :

$$\left. \begin{aligned} \text{Ms}_T &= \varepsilon_T \cdot L_T^c + \rho_{T,S=80\text{ K}} \cdot L_{TW}^c \\ \text{Mb}_T &= L_T^c \end{aligned} \right\} \quad (10)$$

and we can study the influence of the various assumptions stated to determine total emissivity from our measurements.

To evaluate the error made by the assumption $\rho_{T_A} = \rho_{T_B}$, we introduce the model values of Ms_T and ε_{T_A} in Eq. (5) to determine ε_{T_B} and we compare with the modeled emissivity at T_B . The resulting errors are shown for $B = 10^{-5}$ (Fig. 3).

We estimate the error due to the other assumptions made for the two methods when $\rho_{T_A} = \rho_{T_B}$ (Fig. 4). The error is always “in excess”. The “iterative differential method” looks better than the “differential method at the lowest temperature”, but the reverse is true if we introduce noise levels that are of the same order of magnitude as the radiant energy to be measured. The resulting error is less than 0.5% for temperatures above 40 K and remains negligible for temperatures higher than 80 K. An example of results for “iterative differential method” is reproduced in Table 1 below.

We shall then consider the different sources of experimental errors. The main causes of experimental errors are:

- (1) a variation of the background (temperature stability of the “vacuum chamber” and the Au optics).
- (2) an error on the blackbody (reference) emissivity value: $\leq 0.4\%$.

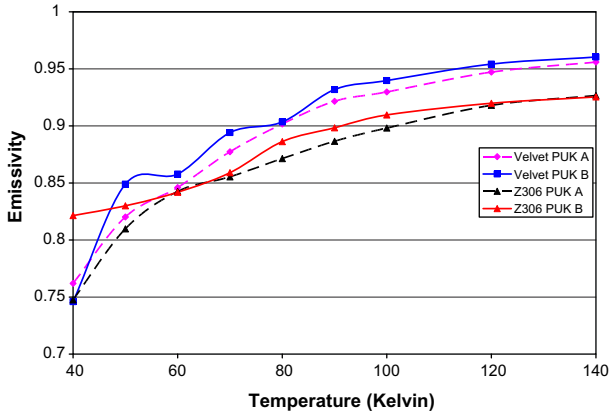


Fig. 6. Run-to-run errors emissivity errors due to the uncertainty of measurement (the repeatability of the process).

- (3) the relative average deviation of the measured electrical signal due to the electronic noise of the measuring equipment: $\pm 0.05\%$ of the measured signal at 40 K and practically negligible above 60 K.
- (4) differences in temperature between the samples disposed on the holder and the blackbody. We found that these differences were less than 0.1 K.

We used thermocouples to check the temperature stability of the vacuum chamber and of the optics. We could observe a very good temperature stability of the pieces of equipment during the measurement process. For instance, the temperature measured for the inner surface of the double wall in the vacuum chamber is 80 K with a less than $\pm 0.2\%$ variation when the sample temperature is below 60 K. Above 60 K, the influence of the background radiation reduces very quickly.

To figure out the uncertainties due to all these perturbations, we took the simulated measurement with $B = 10^{-5}$ and we added random perturbations to the corresponding measured intensities. Then we introduced back in equation system Eq. (10) the disturbed intensity values to derive emissivity by the differential method. In Fig. 5, we represented the global error. The error on emissivity is about 2% for 60 K and still acceptable for lower temperatures.

In Fig. 6 we show the results of measurements realized on two different samples of the same coatings, respectively Velvet and Z306 A and B. The dispersion of results is coherent with the estimation of global errors. Moreover, looking at the curve aspect gave us a good confidence concerning the repeatability of the process.

5. Measurements and results

In order to avoid multiple reflections between the sample and the detection optics, we measured the signals at a minimum angle of 20° with the normal to the sample surface. For complete results, we measured the emissivities for several angles between 20° and 60° (Fig. 7).

For a 20° angle and a sample temperature stabilized at 20 K, typical results are shown in Fig. 8. Even for such a low temperature we observe significant differences between all samples, which means that the sensitivity of our measuring equipment is good. On Fig. 8, for the lowest temperature, we mainly detect the reflected signal from the samples. So a higher signal value means a lower emissivity value. We can verify that our blackbody is effectively less reflective than the coatings.

The results obtained for the total emissivity of the different coatings are reproduced. As discussed above, the results are ob-

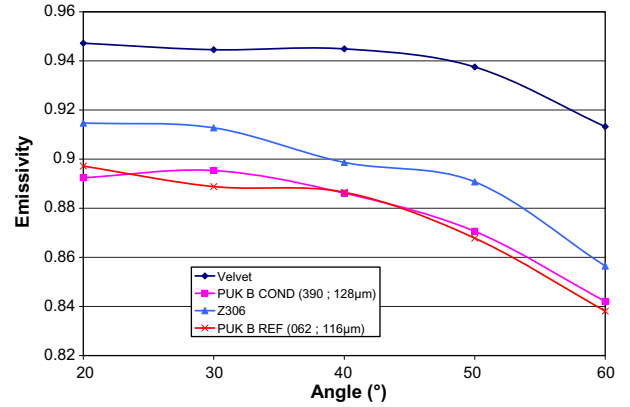


Fig. 7. Angular total emissivities obtained by the differential method.

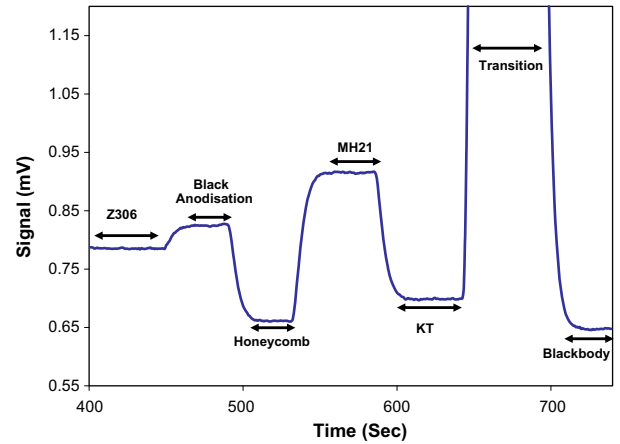


Fig. 8. Example of signals recorded for several samples at 20 K (KT: Kayser-Threde).

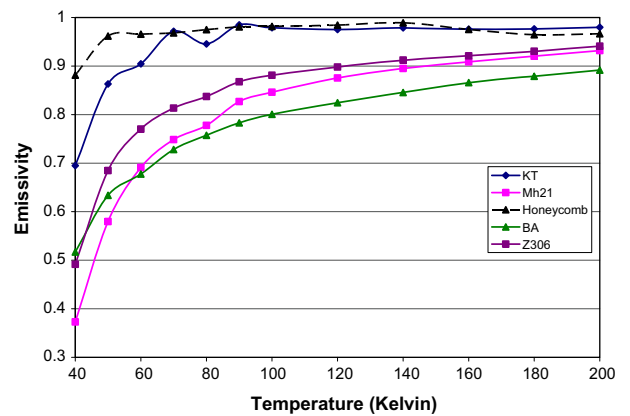


Fig. 9. Emissivities at 20° of different coatings obtained by the differential method (KT: Kayser-Threde; BA: Black Anodisation).

tained with about $\pm 4\%$ error at 40 K. For temperatures higher than 60 K, the accuracy is much better and the cumulated error does not exceed 3%. We then classify the coatings following their emissivity. We made some repetitivity measurements that confirm our error calculations (Fig. 5).

As we can dispose five samples at the same time on the holder, we wanted to check that the results are not influenced by the

position of the samples. So, we repeated the experiment after changing the order of the samples. The results have a lower dispersion than that due to repetitivity. We then concluded that the position of the sample does not influence measurements.

It clearly appears in Fig. 9 that emissivity decreases with temperature for all coatings and the lowest temperatures part of the curves is very similar for all coatings. Obviously, the lower the temperature the higher the measurement error, but the smooth appearance of the curves suggests that the measurement error is small enough not to hide the underlying physical phenomenon. The coatings studied are thin dielectric films disposed on copper or aluminium substrate. At low temperatures, the global radiated power is located in the far infrared where the coatings become transparent. The energy measured corresponds then to the radiation of the metallic substrate through a more and more transparent layer.

6. Conclusions and future prospects

The described work was aimed to obtain the total directional emissivity at cryogenic temperatures of various dielectric coatings disposed on metallic substrate. The results give ESA the capability to choose the most efficient coating in order to cool the Planck satellite baffle and to calculate the equilibrium temperature close to the telescope.

The main flaws of the measurement process were due to the background radiations inside the vacuum chamber that reflect on the sample. We constantly tried to reduce the sources of errors by improving the experimental setup. Using the "iterative differential method" and using a very precise regulation of the chamber wall, we obtained a drastic reduction of the influence of the most obvious perturbations. However, after each improvement step, new perturbations appeared that were previously hidden.

A new improvement could result from cooling the double wall with liquid helium instead of liquid nitrogen. The color temperature of the background could then get down and stabilise around 30 K instead of 80 K. We could also dispose the chopper motor and the bolometer inside the chamber.

We are often questioned about direct spectral emissivity measurements at cryogenic temperatures. We already conducted such experiments at as low temperatures as 200 K. With the identified improvements to the experimental setup, we can foresee to study the spectral emissivity of dielectric materials at the same levels of temperatures as those considered here. Such measurements could then be done using the bolometer in association with a Fourier Transform Spectrometer.

References

- [1] Collaudin B, Rando N. Cryogenics in space: a review of the missions and of the technologies. *Cryogenics* 2000;40:797–819.
- [2] Francou L, Hervé P. An FTIR based instrument for measuring infrared diffuse reflectance. Quantitative infrared thermography (QIRT 1998), Eurotherm Seminar no. 60, Lodz Pologne; 7–10 September 1998.
- [3] Mattei S, Especel D. Une méthode de mesure de l'émissivité thermique des matériaux opaques à la température ambiante. *Revue générale de la thermique* 1994;33(8):239–58.
- [4] Fabron C. Measurement of total hemispheric emissivity at low temperatures – designing a cryogenic test bench. In: Intal conference on environmental systems; July 2000, Toulouse France, Publication SAE 2000-01-2526.
- [5] Musilova V, Hanzelka P, Kralik T, Srnka A. Low temperature properties of materials used in cryogenics. *Cryogenics* 2005;45(8):529–36.
- [6] Delouard P, Krähenbühl U, G. Peikert G. Materials characterisation at cryogenic temperatures for the Planck telescope. In: European conference on spacecraft structures, materials & mechanical testing 2005, Noordwijk, The Netherlands; 10–12 May 2005. Publication ESA, SP-581; August 2005.
- [7] Te Y, Jeseck P, Camy-Peyret C, Payan S, Briauudeau S, Fanjeaux M. High emissivity black body for radiometric calibration near ambient temperature. *Metrologia* 2003;24–30(40).